Photodiagnosis and Photodynamic Therapy 55 (2025) 104738

Contents lists available at ScienceDirect

Photodiagnosis and Photodynamic Therapy

journal homepage: www.elsevier.com/locate/pdpdt

Research Paper

Biofluorescence imaging as a valid alternative for dental calculus detection

Sun-Young Lee [a,1], Hyung-Suk Lee [b,1], Eun-Song Lee [b], Hoi-In Jung [b], Baek-Il Kim [b,*]

[a] Department of Dental Hygiene, Sahmyook Health University, Seoul, , Republic of Korea
[b] Department of Preventive Dentistry & Public Oral Health, BK21 FOUR Project, Yonsei University College of Dentistry, Seoul, Republic of Korea

ARTICLE INFO

Keywords:
Dental calculus
Red biofluorescence
Biofluorescence imaging
Calculus detection
Color difference

ABSTRACT

Background: Dental calculus is a major contributor to periodontal disease, and its effective removal depends on accurate detection. This study aimed to evaluate the detectability of dental calculus using quantitative biofluorescence imaging (BFI) and to assess its diagnostic accuracy compared to white-light imaging (WLI) and conventional visual-tactile (VT) examination.

Methods: Ten adults were enrolled, and 100 tooth surfaces from the buccal side of maxillary molars and the ligual side of mandibular anterior teeth were examined at three sites (mesial, central, distal), yielding 300 sites. After excluding 15 unsuitable sites, 285 were analyzed. Each site was imaged using WLI and BFI with a biofluorescence-enabled intraoral camera (Qraypen C®, AIOBIO, Korea). VT examination served as the reference standard, and sites were categorized as No calculus, Initial calculus, or Advanced calculus. Color difference (ΔE) and red biofluorescence intensity (ΔR) were measured. Diagnostic accuracy, including sensitivity, specificity, false-positive, and false-negative rates, was compared between imaging modalities.

Results: BFI showed significantly higher ΔE values than WLI, with values increasing by calculus severity ($p < 0.001$). ΔR also rose with accumulation: 2.75% (No calculus), 6.06% (Initial), 15.58% (Advanced). Detection accuracy improved with WLI + BFI versus WLI alone: sensitivity (0.84 vs. 0.61), specificity (1.00 vs. 0.91), and false-negative rate (16.1% vs. 38.7%).

Conclusion: Biofluorescence imaging enables more distinct detection of dental calculus than white-light imaging, with higher sensitivity and specificity. This method not only identifies calculus presence but also allows quantitative assessment of its accumulation, enhancing diagnostic accuracy.

1. Introduction

Dental calculus is a calcified dental biofilm that forms within the oral cavity and adheres firmly to the surfaces of natural teeth and dental prostheses [1]. Its formation begins with bacterial attachment to the acquired pellicle, followed by biofilm maturation and subsequent mineralization through the deposition of calcium and phosphate ions present in saliva [2]. During this process, various calcium phosphate crystals, including hydroxyapatite, are formed, and the calculus structure becomes porous, incorporating pathogenic bacteria and endotoxins [1,3,4]. Due to these biological characteristics, dental calculus is not merely a mineralized deposit but serves as a reservoir of pathogenic microorganisms and inflammatory mediators. It acts as a significant secondary etiological factor that continuously irritates the gingival tissues and contributes to the onset and progression of periodontal disease [5].

Traditionally, dental calculus has been detected through visual inspection, tactile examination, and radiographic imaging [6]. Among these, visual inspection is a simple method relying on the examiner's observation of color and morphology with the naked eye. However, its accuracy is limited due to the subjective nature of the assessment and strong dependence on the examiner's experience and skill level [7]. Additionally, the appearance of calculus varies depending on factors such as deposition duration, dietary habits, and oral hygiene, making it difficult to distinguish from sound tooth surfaces of similar color. It may also be confused with surface gloss or other deposits, further complicating accurate identification [2,6]. Tactile examination involves the use of a periodontal probe to physically detect the rough surface of calculus and is useful for identifying subgingival deposits not visible to the eye [8]. However, this method depends on the clinician's tactile

* Corresponding author.
E-mail addresses: isy078@shu.ac.kr (S.-Y. Lee), ianhslee@yuhs.ac (H.-S. Lee), eunsong@yuhs.ac (E.-S. Lee), junghoiin@yuhs.ac (H.-I. Jung), drkbi@yuhs.ac (B.-I. Kim).
[1] These authors contributed equally to this study.

https://doi.org/10.1016/j.pdpdt.2025.104738
Received 10 May 2025; Received in revised form 6 July 2025; Accepted 25 July 2025
Available online 25 July 2025

sensitivity, which can lead to variability and inconsistency in results [8, 9]. Radiographic examination is effective for detecting calculus in non-visible areas, but is limited in identifying fine deposits, cannot detect calculus on buccal or lingual surfaces, and requires a high level of interpretative skill for accurate diagnosis [9,10]. Despite their clinical utility, these conventional methods are primarily qualitative and limited in objectivity and in quantitatively assessing calculus accumulation. Early detection and quantitative evaluation are essential for preventing periodontal disease; however, existing methods are particularly inadequate for detecting early-stage calculus.

To overcome the limitations of conventional detection methods, biofluorescence technology has recently been introduced in dentistry as a noninvasive imaging tool to improve diagnostic accuracy and monitor treatment progress [11]. This technique is based on the principle that oral tissues absorb blue visible light in the wavelength range of approximately 400–450 nm and subsequently emit fluorescence at longer wavelengths (green or red) as the energy decreases [12–14]. Dental calculus, in particular, is not merely a mineralized structure but also contains bacterial metabolites such as porphyrins, which emit red biofluorescence in the 600–700 nm [15]. This biofluorescence behavior was previously reported in a spectroscopic study, which confirmed strong emission from dental calculus under short-wavelength excitation [16]. In contrast, sound tooth structures exhibit green biofluorescence between 460 and 560 nm, allowing for clear differentiation between the calculus and surrounding tissues. Therefore, calculi that may be difficult to identify visually or through tactile examination can be objectively detected using red biofluorescence patterns. Biofluorescence technology has the potential to reduce the examiner-dependent variability associated with conventional methods and compensate for the challenges of detecting early-stage calculus. Because the biofluorescence characteristics of dental calculus allow visualization of its distribution and accumulation in a quantifiable manner, this technique may enhance the diagnostic accuracy of calculus detection compared to traditional methods [17].

However, existing studies have primarily focused on analyzing the red biofluorescence characteristics of dental biofilm [18,19], while quantitative evaluations of the biofluorescence intensity or distribution of dental calculus itself remain limited [15,18,20]. In addition, most previous studies on calculus detection have relied on qualitative assessments of its presence or absence, resulting in diagnostic outcomes still largely dependent on the clinician's subjective judgment [21,22]. Therefore, it is necessary to objectively and quantitatively analyze the inherent biofluorescence characteristics of dental calculus and to develop a new detection method applicable in clinical practice based on these findings [23,24]. This approach may enable more objective and intuitive detection of calculus, helping minimize unnecessary interventions and facilitating efficient deposit removal—ultimately improving the efficiency of scaling procedures and the overall quality of periodontal treatment.

Therefore, this study aimed to investigate whether biofluorescence technology can be used to assess both the presence and accumulation level of dental calculus. Accordingly, color differences between calculus and sound tooth structures were analyzed and compared between white-light and biofluorescence images. In addition, based on visual-tactile examination results, the diagnostic accuracy of calculus detection was compared between assessments using white-light images and those based on biofluorescence evaluation.

2. Materials and methods

2.1. Study design

This study was conducted to quantitatively analyze the color characteristics and biofluorescence response of dental calculi to evaluate the diagnostic accuracy and clinical applicability of biofluorescence technology for calculus detection. This study was conducted from July 2020 to June 2021 at the Clinical Dental Hygiene Laboratory of a university in Seoul, Republic of Korea. This study was approved by the Institutional Review Board (IRB No. 116286–202006-HR-02) and conducted in accordance with the ethical principles of the Declaration of Helsinki.

Sites with visible calculus in the oral cavity of participants meeting the inclusion criteria were imaged using a biofluorescence-based device to obtain both white light and biofluorescence images. Two trained examiners performed visual tactile (VT) examinations to determine the presence or absence of calculi. Based on the VT results, each site was classified into one of the three groups according to the degree of calculus accumulation: No calculus, Initial calculus, or Advanced calculus. Color differences (ΔE) and biofluorescence parameters (ΔR) were calculated and compared across the three groups. VT examination was used as the gold standard to evaluate the diagnostic accuracy of calculus detection using both white light and biofluorescence images (Fig. 1).

2.2. Participants selection

Participants were healthy adults aged 19–65 years who had no systemic diseases and voluntarily agreed to participate after receiving both written and verbal explanations of the study's purpose and procedures. Eligible participants had 28 natural teeth, excluding third molars, and had not undergone scaling or calculus removal within the past year. The exclusion criteria included the use of antibiotics within one month prior to the study, pregnancy or lactation, presence of severe oral pathological conditions (e.g., oral cancer or significant inflammation), advanced periodontal disease, or extensive dental caries.

2.3. Selection of teeth and evaluation sites

A preliminary oral examination was conducted on 25 initially recruited participants (21 males and 4 females; mean age: 22.6 $\pm$ 6.2 years). Of these, 10 participants (7 males and 3 females; mean age: 22.8 $\pm$ 6.8 years) were ultimately selected based on the absence of restorations on the evaluation teeth and fulfillment of the inclusion criteria. The target teeth were chosen from regions adjacent to salivary gland openings—areas prone to active mineral deposition and often missed during routine oral hygiene. Accordingly, 10 natural teeth were selected per participant: the maxillary right and left first and second molars, and the mandibular right and left central incisors, lateral incisors, and canines. From these, the buccal surfaces of the maxillary molars and the lingual surfaces of the mandibular anterior teeth—sites with a high prevalence of calculus formation—were designated as evaluation areas, yielding 100 tooth surfaces (40 maxillary and 60 mandibular anterior lingual surfaces). Each surface was further divided into three sections (mesial, central, and distal) based on anatomical landmarks, resulting in 300 evaluation sites for analysis. The presence or absence of calculus at each site was determined by VT examination, followed by quantitative analysis.

2.4. Acquisition of calculus images

Calculus imaging was performed under standardized conditions by a single examiner, following a consistent protocol. Prior to imaging, tooth brushing was performed to remove food debris, material alba, and dental biofilms, thereby minimizing external factors that could affect the analysis. Using the Qraypen C® (AIOBIO, Seoul, Republic of Korea), white-light (WLI) and biofluorescence images (BFI) were captured sequentially. The device automatically captured images in sequence using an autofocus function. First, the white LED was activated to acquire the WLI. Then, a short-wavelength excitation light centered at 405 nm was used to acquire the BFI [25,26]. This visible blue-violet light induces red biofluorescence from calculus, enhancing visual differentiation. The camera was positioned as perpendicular to the tooth surface as much as possible to ensure proper visualization of the mesial, central, and distal areas of each surface. All images were acquired with the

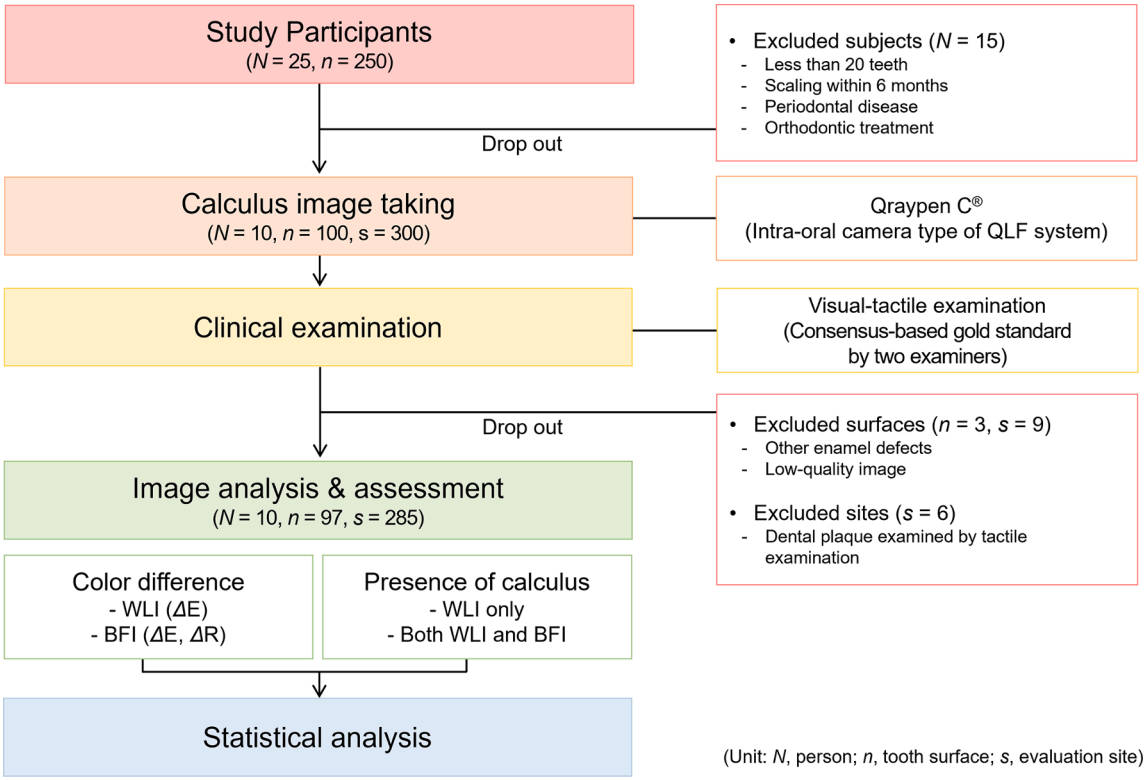

Fig. 1. Flow diagram of the dental calculus quantification process.

participants seated in a dental unit chair within the same clinical laboratory. Interference from ambient light was minimized using blackout curtains and blocking external illumination. The soft tissues and lips were retracted using a cheek retractor and dental mirror, and moisture was removed using a 3-way syringe to enhance image clarity.

2.5. Visual-tactile (VT) examination

Following image acquisition, two experienced examiners independently performed VT examinations using a periodontal probe. The presence and distribution of calculus at each evaluation site were recorded. The location of calculus deposits was documented using a custom-designed "calculus drawing chart," developed for this study. This chart reflected the anatomical structure of the tooth, dividing each surface into three regions—mesial, central, and distal—to allow precise recording of localized calculus distribution. In cases where the examiners' assessments differed, a consensus process was conducted to resolve discrepancies and ensure consistency and reliability in the final evaluation results.

2.6. Classification of calculus

Previous studies on calculus detection have often relied on either visual inspection or tactile examination alone [6,21,23]. In contrast, the present study employed a combined VT examination to achieve a more accurate assessment. Based on the VT results, the degree of calculus accumulation was classified into three categories according to operational definitions: 'No calculus,' 'Initial calculus,' and 'Advanced calculus.' The VT examination results obtained through this procedure were established as the gold standard in this study and served as the

VT calculus classification	Description	Image	Tactile chart
No calculus	Smooth surface No suspected deposit		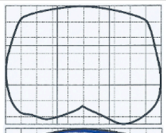
Faint visible calculus	Rough surface detectable by tactile examination but not visually apparent deposit		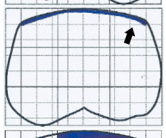
Distinct visible calculus	Rough surface detectable by tactile examination and visually apparent deposit		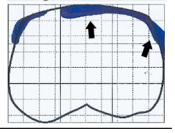

Fig. 2. Visual-tactile (VT) classification of dental calculus with representative images and tactile chart annotations. Black arrows indicate the location of the calculus on the tooth surface as confirmed by VT examination.

reference for the subsequent quantitative analysis and comparison of detection accuracy. The definitions of each calculus category, along with representative examples of WLIs and VT chart recordings, are presented in Fig. 2.

2.7. Image selection and area of interest (AOI) designation

A dataset was constructed by selecting WLIs and BFIs that matched the anatomical structure of the gold standard chart to quantitatively analyze the color difference between dental calculus and sound tooth surfaces based on the presence or absence of calculus. The selected images were cropped and aligned according to the chart structure, and tooth positions were standardized for consistent use in subsequent analyses (Fig. 3). For each participant, 10 WLIs were collected under white light and 10 BFIs were collected under biofluorescence, resulting in a total of 20 images per subject. Each tooth surface was divided into three regions—mesial, central, and distal—yielding 300 evaluation sites. Area of interest (AOIs) were designated using the ImageJ software (version 1.51j, National Institutes of Health, Bethesda, MD, USA). Based on the gold standard chart, patches were placed over regions with confirmed calculi and saved as AOIs. The same AOIs were then applied to both the WLIs and BFIs. For the sound areas, adjacent calculus-free regions were selected and the patch lengths matched those of the calculus areas. To ensure consistency, the AOIs were designated within the same surface, while considering the optical conditions and surface characteristics.

2.8. Color difference analysis

The CIELAB color space system was used to quantitatively analyze the color differences between the calculus and sound tooth surfaces in both WLIs and BFIs [27,28]. For each area of interest (AOI), L^* (lightness), a^* (red–green), b^* (yellow–blue) values were extracted based on predefined analysis patches. The same AOIs were applied to both WLIs and BFIs to ensure consistency. Color difference (ΔE) between the two regions was calculated using the following formula [28,29]:

$$\Delta E = \sqrt{\left(L^*_{calculus} - L^*_{sound}\right)^2 + \left(a^*_{calculus} - a^*_{sound}\right)^2 + \left(b^*_{calculus} - b^*_{sound}\right)^2}$$

A ΔE value of 1 or higher is generally perceptible to the human eye, and in dental clinical settings, a value of $\Delta E \geq 3.7$ is commonly considered a clinically meaningful color difference [30,31]. In this study, ΔE values were calculated separately for WLIs and BFIs. In addition, for the BFIs, a red biofluorescence intensity difference (ΔR) was also computed to reflect the relative strength of red biofluorescence [28,32]. To calculate ΔR, red (R) and green (G) values were extracted from each AOI in the RGB color space, and the difference in the red-to-green ratio between the calculus and sound regions was calculated using the following formula:

$$\Delta R\ (\%) = \frac{(R/G)_{calculus} - (R/G)_{sound}}{(R/G)_{sound}} \times 100$$

2.9. Image assessment for calculus detection

To compare the performance of image-based calculus detection, two conditions were established: (1) white-light image (WLI) only and (2) WLI combined with biofluorescence image (BFI). Two examiners independently assessed the presence or absence of calculi under each imaging condition. In cases of disagreement, the final detection result was determined by consensus. The consensus results were then compared with the gold standard, defined by VT examination, to evaluate the accuracy of calculus detection under each imaging condition. Based on this comparison, the differences in the detection accuracy according to the imaging method were analyzed.

2.10. Statistical analysis

Statistical analyses were performed to evaluate the results of color-difference measurements and image-based calculus detection. The color difference variables (ΔE and ΔR) extracted from WLIs and BFIs were tested for normality using the Kolmogorov-Smirnov test. As the data were not normally distributed, the Kruskal-Wallis test was used to compare ΔE and ΔR values among three calculus groups (No calculus, Initial calculus, and Advanced calculus). When statistically significant differences were found, *post-hoc* analysis was performed using the Mann-Whitney U test with Bonferroni correction. To evaluate image-based calculus detection, the results from two conditions—WLI only and WLI with BFI—were analyzed. Following independent assessments by two examiners under each condition, the consensus results were compared with the gold standard defined by the VT examination. Based on this comparison, the sensitivity, specificity, false-positive rate, and false-negative rate were calculated for each image assessment condition. All statistical analyses were performed using SPSS software (version 23.0; SPSS Inc., Chicago, IL, USA), with a significance level set at $\alpha = 0.05$.

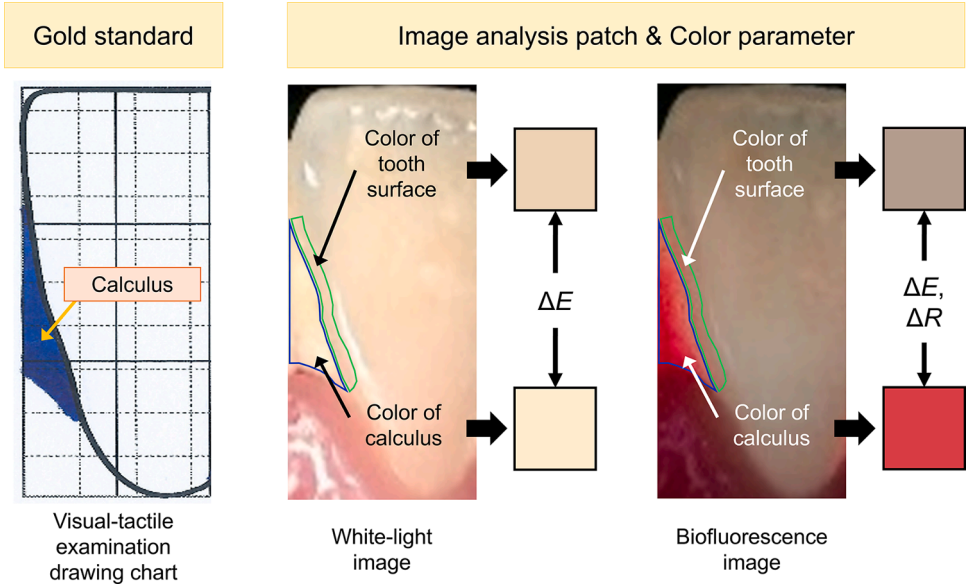

Fig. 3. Color difference analysis (ΔE, ΔR) of dental calculus using image patches defined by gold standard localization.

Table 1
Color difference (ΔE) according to calculus classification in white-light and biofluorescence images.

VT calculus classification	*N* (%)	White-light image	Biofluorescence image	
		ΔE	ΔE	ΔR (%)
No calculus	55 (19.3)	2.68[a] (2.08, 4.14)	3.20[a] (2.63, 4.66)	2.75[a] (1.97, 4.12)
Initial calculus	89 (31.2)	4.21[b] (2.90, 5.81)	5.88[b] (4.33, 9.90)	6.06[b] (4.11, 12.48)
Advanced calculus	141 (49.5)	3.80[b] (2.49, 5.89)	11.52[c] (7.34, 18.15)	15.58[c] (9.25, 28.71)
P-value		< 0.001	< 0.001	< 0.001

Data are median (first, third quartile) values.
Different letters (a-c) within the same column indicate significant differences between the calculus groups by the Kruskal-Wallis test and Mann-Whitney U test with Bonferroni *post-hoc* correction.
VT, visual-tactile examination.

3. Results

A total of 100 tooth surfaces were evaluated from 10 study participants, and each surface was divided into three regions (mesial, central, and distal), resulting in 300 evaluation sites. Among these, 15 sites were excluded on the basis of the VT examination results because they were identified as dental biofilms rather than calculi. Finally, 285 sites were included in the final analysis. Of these, 55 sites (19.3%) were classified as having no calculi, whereas 230 (80.7%) were identified as having calculi. Among the calculus-positive sites, 89 (31.2%) were classified as initial calculi and 141 (49.5%) as advanced calculi according to the VT calculus classification criteria (Table 1).

On WLI, sites without calculus (No calculus) exhibited a smooth surface with retained gloss, and the color was consistent with the adjacent sound enamel areas (Fig. 4). Sites classified as Initial calculus showed surface characteristics similar to those of sound areas. In some regions, a slight loss of gross or suspected roughness was noted, but no distinct color differences were observed. In contrast, sites with Advanced calculus clearly displayed rough surfaces with visually distinct deposits in white or yellowish tones, forming defined boundaries. In BFI, Initial calculus sites showed localized red biofluorescence that was not visible under white light observation. Advanced calculus sites exhibit strong red biofluorescence in the calculus-affected areas, presenting a clear color contrast from the surrounding sound surfaces.

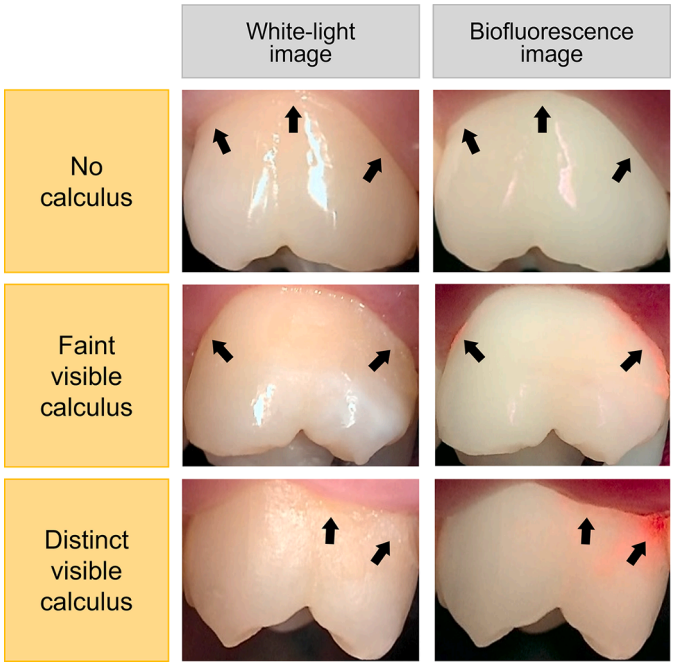

Fig. 4. Representative white-light and biofluorescence images of teeth categorized according to the visual-tactile (VT)-based calculus classification. Arrows indicate the evaluation sites on each tooth surface. The three categories were classified based on the VT gold standard.

The ΔE value, a quantitative indicator of color difference between calculus sites and adjacent sound areas, showed statistically significant differences among the three VT calculus classification groups in both WLIs and BFIs ($p < 0.001$, Table 1). In WLIs, the Initial calculus group exhibited the highest ΔE value (4.21), and no statistically significant difference was found between the Initial and Advanced calculus groups. In contrast, in the BFIs, the ΔE values increased progressively from the No calculus group (3.20) to the Initial calculus group (5.88) and the Advanced calculus group (11.52), with all pairwise comparisons showing statistically significant differences ($p < 0.001$). Additionally, within each calculus group, ΔE values were higher in BFIs than in WLIs, and this difference tended to increase with the severity of calculus. Notably, in the Advanced calculus group, the ΔE value in BFIs was approximately three times higher than that in WLIs.

The ΔR value, a quantitative indicator of the difference in red biofluorescence intensity between calculus sites and adjacent sound areas, showed statistically significant differences among the three VT calculus classification groups in BFIs ($p < 0.001$, Table 1). The ΔR value was lowest in the No calculus group (2.75%) and increased progressively in the Initial calculus (6.06%) and the Advanced calculus group (15.58%). Compared to the No calculus group, the ΔR value was approximately 2.2 times higher in the Initial calculus and 5.7 times higher in the Advanced calculus group than in the No calculus group. In addition, as the degree of calculus accumulation increased, the range of ΔR values tended to widen, indicating greater variability in red biofluorescence intensity within the Advanced calculus group.

A comparison of the calculus detection performance between the WLI-only condition and the combined WLI and BFI conditions revealed a clear difference between the two approaches (Table 2). Among the 230 calculus-positive sites identified based on the VT gold standard, 193 (83.9%) were detected under WLI with BFI, whereas only 141 (61.3%) were detected under WLI-only. Of the 55 calculus-free sites, false-

Table 2
Diagnostic performance by imaging modality for dental calculus detection.

Imaging modality	Detection performance			
	Sensitivity	Specificity	False-positive rate (%)	False-negative rate (%)
WLI-only	0.61	0.91	9.1	38.7
WLI with BFI	0.84	1.00	0.0	16.1

Calculus detection was based on the visual-tactile examination as the reference standard.
Sensitivity and specificity were calculated for each imaging modality.
WLI, white-light image; BFI, biofluorescence image.

positive detections occurred at 5 sites (9.1%) under the WLI-only condition, whereas no false positives were observed under the WLI with BFI condition. The sensitivity and specificity of the WLI with BFI condition were 0.84 and 1.00, respectively. The false-negative rate was 16.1% for WLI with BFI and 38.7% for WLI-only, whereas the false-positive rates were 0.0% and 9.1%, respectively.

4. Discussion

This study aimed to quantitatively evaluate the presence and accumulation of dental calculus using biofluorescence technology and to examine the diagnostic accuracy and clinical applicability of biofluorescence image-based calculus detection by comparing it with white-light imaging. To address the limitations of conventional assessment methods, which primarily consider the quantity of calculus and overlook qualitative changes, calculus was operationally classified into initial and advanced stages. Traditional visual-tactile examination methods often fail to detect early-stage calculus immediately after deposition [6,33,34], thereby hindering early diagnosis and preventive intervention. In this study, calculus was categorized based on qualitative changes observed during formation and mineralization—particularly surface texture and color characteristics—and the efficacy of biofluorescence imaging in detecting not only advanced but also Initial calculus was evaluated according to this operational definition. Quantitative analysis of color difference (ΔE) and red biofluorescence intensity (ΔR) revealed statistically significant differences in both variables according to the presence and severity of calculus in BFIs. These findings demonstrate that biofluorescence-based detection offers superior diagnostic performance compared to conventional visual and tactile examinations and may serve as a reliable and objective tool for calculus detection in clinical practice. Furthermore, this quantitative approach extends beyond the binary classification of calculus presence and proposes a novel diagnostic framework capable of stratifying and objectively assessing the condition of dental calculus. This represents a meaningful contribution from both academic and clinical perspectives.

In this study, an operational definition of dental calculus was established by classifying it into three categories—No calculus, Initial calculus, and Advanced calculus—based on the degree of accumulation. This classification was designed to enable a more refined evaluation of calculus and to systematically assess the sensitivity and specificity of biofluorescence-based detection. Previous studies have largely relied on binary assessments of calculus presence or absence, limiting their ability to detect early or marginal deposits. In contrast, the present study proposes a clinically relevant classification system based on parallel visual-tactile (VT) examinations that considers both the visibility and structural characteristics of calculi. This operational definition served as a quantitative basis for comparing groups in the analysis of image-based ΔE and ΔR values, providing a foundation for objectively evaluating detection sensitivity according to calculus severity. Notably, the significantly higher ΔR values observed in the Initial calculus group compared to the No calculus group suggest that biofluorescence technology has the potential to quantitatively detect early-stage calculus that may not be distinguishable through visual or tactile means. Furthermore, the highest ΔR values recorded in the Advanced calculus group support the validity of this classification system in reflecting the correlation between calculus accumulation and image-derived fluorescence signals. Overall, the operational definition employed in this study goes beyond simple presence or absence identification and offers a meaningful framework for differentiating between the maturity and qualitative characteristics of dental calculi. This may serve as a foundation for developing future diagnostic algorithms linked to the pathophysiological properties of calculus. Additionally, this classification system has practical implications for both clinical and educational settings, where accurate detection and personalized feedback are essential for effective calculus management.

According to the findings of this study, tooth surfaces with calculus appeared primarily yellowish or whitish under WLIs, making it difficult to visually distinguish between Initial and Advanced calculus (Fig. 4). Consistent with this observation, the ΔE analysis under WLIs revealed no clear differences among the three calculus groups, and no statistically significant difference was found between the Initial and Advanced calculus groups (Table 1). Moreover, the ΔE values under WLIs were close to 3.7, the clinically accepted threshold for perceptible color differences, indicating that WLI alone has limited ability to quantitatively distinguish the presence or severity of calculus [30,31]. In contrast, under BFIs, calculus-affected areas exhibited distinct red biofluorescence that clearly differentiated them from sound surfaces. The corresponding ΔE values increased significantly with the degree of calculus accumulation (Table 1). Notably, the ΔE value for the Initial calculus group was approximately three times higher under BFIs than under WLIs, suggesting the technique's effectiveness in detecting early-stage deposits not easily visible to the naked eye. These results indicate that biofluorescence imaging enables not only the detection of calculus presence but also the quantitative differentiation of its accumulation level—based on the operational definition—reflecting qualitative differences in the deposit.

In BFIs, dental calculus is visualized as red biofluorescence. This study quantified the intensity of this fluorescence response by analyzing the ΔR value. The results showed that ΔR significantly increased with the degree of calculus accumulation, with the highest values observed in the advanced calculus group. Compared to the No calculus group, the ΔR value was approximately 2.2 times higher in the Initial calculus group and 5.7 times higher in the Advanced calculus group. Importantly, ΔR significantly distinguished Initial calculus from sound surfaces, suggesting that biofluorescence-based analysis can detect early-stage calculus that is often not identifiable through visual inspection alone. The primary cause of this red biofluorescence is porphyrin metabolites produced by late-colonizing bacteria during the heme biosynthesis pathway within oral biofilms [35,36]. These porphyrins emit strong red fluorescence when excited with blue light near 405 nm [37,38]. Since dental calculus is a calcified form of biofilm, the concentration of these fluorescent metabolites [39] progressively increases during its formation and accumulation. The structural features of dental calculi were found to enhance the fluorescence signals by promoting the accumulation of porphyrin-based metabolites. Dental calculus is a mineralized structure composed of inorganic components, primarily hydroxyapatite, carbonate-substituted apatite, and organic matter [40,41]. Its porous architecture provides a favorable environment for the accumulation and retention of bacterial metabolites [5], which may become fixed or concentrated within the structure over time. In addition, the inorganic minerals deposited during calcification may serve as a matrix that absorbs or stabilizes porphyrin molecules, thereby enhancing the intensity and persistence of the fluorescence response [15,20]. Therefore, the increase in ΔR reflects not only the presence of bacterial activity or biomass but also structural changes within the calculus and the retention of fluorescence-emitting metabolites. From this perspective, ΔR may serve as a potential indicator of calculus maturity and pathogenic accumulation [12,18,42,43].

In this study, the diagnostic accuracy of calculus detection under two image assessment conditions—WLI-only and WLI with BFI—was compared using the VT examination as the reference standard. The validity of the biofluorescence-assisted method was evaluated based on sensitivity, specificity, false-positive rate, and false-negative rate. The analysis demonstrated that the WLI with BFI condition provided superior detection performance compared to that provided by WLI-only. Sensitivity for WLI with BFI was 0.84, approximately 1.4 times higher than that of WLI-only (0.61), and the false-negative rate was 16.1%, less than half that observed under the WLI-only condition (38.7%). Because red biofluorescence is selectively expressed at calculus sites in BFIs, the likelihood of visual confusion due to enamel color or anatomical features is greatly reduced. This was supported by a false-positive rate of 0% under the WLI with BFI condition, indicating no misidentification of

sound surfaces as calculus. In contrast, the WLI-only condition showed a false-positive rate of 9.1%, likely resulting from visual misinterpretation of similarly colored tooth surfaces or anatomical shadows. This highlights the limitations of WLI-only, particularly in detecting early-stage deposits such as Initial calculus, which often have indistinct borders and minimal visual contrast. Without adjunctive tactile input, achieving accurate detection in such cases is challenging. However, WLI with BFI enabled selective visualization of red biofluorescence even in Initial calculus, improving visual detectability. This was further supported by ΔR analysis, which showed significantly higher red biofluorescence intensity in Initial calculus than in sound surfaces. These findings provide scientific evidence that WLI with BFI improves the sensitivity and accuracy of calculus detection and can effectively compensate for the diagnostic limitations of WLI-only approaches.

This study is the first attempt to evaluate the quantitative potential and diagnostic accuracy of biofluorescence-based technology for the detection of dental calculi. Although these findings provide meaningful insights, several limitations should be acknowledged. First, definitive clinical thresholds for interpreting ΔE and ΔR values have not yet been established. In this study, the interpretation was based on the previous literature and the perception of color differences. Future studies are needed to determine clinically applicable cut-off values under diverse clinical conditions. Second, the analysis was limited to 285 areas of interest (AOIs) obtained from a relatively homogeneous sample. Caution should be exercised when generalizing these findings to broader populations or patients with varying clinical conditions. Third, this study used a cross-sectional design that does not capture longitudinal changes in calculus accumulation or responses to treatment over time. Additionally, the influence of physical characteristics, such as hardness, thickness, and mineral content of the calculus, on the biofluorescence intensity was not considered. Further studies should explore the quantitative relationships between the multidimensional properties of calculi and their biofluorescence responses. Lastly, although this study assumed that ΔR values may be associated with pathogenicity, this assumption was based on existing literature rather than direct microbiological evidence. To validate the use of ΔR as an indicator of pathogenic potential, future experimental and clinical studies should investigate its quantitative relationship with microbial composition and inflammatory markers.

This study provides foundational evidence supporting the use of biofluorescence imaging not only in clinical dentistry but also in preclinical dental hygiene education. The visual clarity of BFIs may enhance learners' detection skills and contribute to the development of objective and reproducible assessment systems. This technology also holds considerable potential for expansion into digital educational content, simulation-based learning, and artificial intelligence–driven automated detection systems [44,45]. Future research should include large-scale studies reflecting diverse patient populations and real-world clinical environments, as well as investigations into correlations between the physical properties of calculus and its fluorescence response. Moreover, the clinical validity of ΔR as a predictive indicator of pathogenicity should be examined. As a starting point for such future research, the present study provides valuable insight by introducing a new paradigm for quantifying calculus detection and exploring its application in educational contexts.

5. Conclusion

This study demonstrated that biofluorescence imaging enables clearer differentiation between calculus-affected and sound tooth surfaces than white-light imaging. Quantitative analysis using ΔE (color difference) and ΔR (red biofluorescence intensity) values allowed for the evaluation of fluorescence response according to the degree of calculus accumulation. Notably, biofluorescence imaging is effective in detecting early stage calculi that are difficult to identify visually. In addition, the incorporation of biofluorescence imaging improves the sensitivity and specificity of calculus detection, suggesting its potential as a more precise diagnostic tool in clinical practice.

Clinical significance

Biofluorescence imaging enables clearer visual differentiation of dental calculus by highlighting color differences, allowing objective evaluation and improving diagnostic performance in both clinical practice and dental hygiene education.

CRediT authorship contribution statement

Sun-Young Lee: Writing – review & editing, Writing – original draft, Validation, Methodology, Investigation, Formal analysis, Conceptualization. **Hyung-Suk Lee:** Writing – review & editing, Visualization, Validation, Methodology, Investigation, Formal analysis, Conceptualization. **Eun-Song Lee:** Writing – review & editing, Visualization, Formal analysis. **Hoi-In Jung:** Writing – review & editing, Formal analysis. **Baek-Il Kim:** Writing – review & editing, Supervision, Resources, Project administration, Funding acquisition, Conceptualization.

Declaration of competing interest

The authors declare that they have no competing interest.

Acknowledgements

This research was supported by a grant of the Korea Health Technology R&D Project through the Korea Health Industry Development Institute (KHIDI), funded by the Ministry of Health & Welfare, Republic of Korea (grant number: HI20C0129), and the Bio & Medical Technology Development Program of the National Research Foundation (NRF) and funded by the Korean Government (MSIT) (No. 2022M3A9F3016364, RS-2022-NR067350).

References

[1] R. Forshaw, Dental calculus - oral health, forensic studies and archaeology: a review, Br. Dent. J. 233 (11) (2022) 961–967, https://doi.org/10.1038/s41415-022-5266-7.
[2] S. Jepsen, J. Deschner, A. Braun, F. Schwarz, J. Eberhard, Calculus removal and the prevention of its formation, Periodontol. 2000 55 (1) (2011) 167–188, https://doi.org/10.1111/j.1600-0757.2010.00382.x.
[3] I.D. Mandel, Calculus update: prevalence, pathogenicity and prevention, J. Am. Dent. Assoc. 126 (5) (1995) 573–580, https://doi.org/10.14219/jada.archive.1995.0235.
[4] R.S. Levine, Pyrophosphates in toothpaste: a retrospective and reappraisal, Br. Dent. J. 229 (10) (2020) 687–689, https://doi.org/10.1038/s41415-020-2346-4.
[5] S. Aghanashini, B. Puvvalla, D.B. Mundinamane, S.M. Apoorva, D. Bhat, M. Lalwani, A comprehensive review on dental calculus, J. Health Sci. Res. 7 (2) (2016) 42–50, https://doi.org/10.5005/jp-journals-10042-1034.
[6] S.R. Muglikar, S.R. Dhande, R.V. Hegde, P.S. Ghodke, R.S. Baksh, A. Shaikh, Current strategies for dental calculus detection: a review, Int. J. Dent. Med. Sci. Res 3 (2) (2021) 454–461, https://doi.org/10.35629/5252-0302454461.
[7] J.C. Hyer, D.E. Deas, A.A. Palaiologou, M.E. Noujeim, M.J. Mader, B.L. Mealey, Accuracy of dental calculus detection using digital radiography and image manipulation, J. Periodontol. 92 (3) (2021) 419–427, https://doi.org/10.1002/jper.19-0669.
[8] Y.L. Qin, X.L. Luan, L.J. Bi, Z. Lü, Y.Q. Sheng, G. Somesfalean, et al., Real-time detection of dental calculus by blue-LED-induced fluorescence spectroscopy, J. Photochem. Photobiol. B 87 (2) (2007) 88–94, https://doi.org/10.1016/j.jphotobiol.2007.03.002.
[9] F. Shakibaie, L.J. Walsh, DIAGNOdent Pen versus tactile sense for detection of subgingival calculus: an in vitro study, Clin. Exp. Dent. Res. 1 (1) (2015) 26–31, https://doi.org/10.1002/cre2.5.
[10] T.J. Lin, Y.T. Lin, Y.J. Lin, A.Y. Tseng, C.Y. Lin, L.T. Lo, et al., Auxiliary diagnosis of dental calculus based on deep learning and image enhancement by bitewing radiographs, Bioengineering. (Basel) 11 (7) (2024), https://doi.org/10.3390/bioengineering11070675.
[11] E.S. Lee, H.K. Yim, H.S. Lee, J.H. Choi, J.H. Lee, B.I. Kim, Clinical assessment of oral malodor using autofluorescence of tongue coating, Photodiagnosis. Photodyn. Ther. 13 (2016) 323–329, https://doi.org/10.1016/j.pdpdt.2015.09.001.
[12] E.S. Lee, S.M. Kang, H.Y. Ko, H.K. Kwon, B.I. Kim, Association between the cariogenicity of a dental microcosm biofilm and its red fluorescence detected by

Quantitative light-induced Fluorescence-Digital (QLF-D), J. Dent. 41 (12) (2013) 1264–1270, https://doi.org/10.1016/j.jdent.2013.08.021.
[13] H.S. Lee, S.K. Kim, S.W. Park, E. de Josselin de Jong, H.K. Kwon, S.H. Jeong, et al., Caries detection and quantification around stained pits and fissures in occlusal tooth surfaces with fluorescence, J. Biomed. Opt. 23 (9) (2018) 1–7, https://doi.org/10.1117/1.Jbo.23.9.091402.
[14] H.S. Lee, E.S. Lee, H.I. Jung, B.I. Kim, Red biofluorescence revealed by dental bleaching in discolored pits and fissures of occlusal caries, J. Dent. 156 (2025) 105646, https://doi.org/10.1016/j.jdent.2025.105646.
[15] Y.K. Lee, Fluorescence properties of human teeth and dental calculus for clinical applications, J. Biomed. Opt. 20 (4) (2015) 040901, https://doi.org/10.1117/1.Jbo.20.4.040901.
[16] S. Gonchukov, T. Biryukova, A. Sukhinina, Y. Vdovin, Fluorescence detection of dental calculus, Laser. Phys. Lett. 7 (11) (2010) 812–816, https://doi.org/10.1002/lapl.201010065.
[17] H.J. Guk, E.S. Lee, U.W. Jung, B.I. Kim, Red fluorescence of interdental plaque for screening of gingival health, Photodiagnosis. Photodyn. Ther. 29 (2020) 101636, https://doi.org/10.1016/j.pdpdt.2019.101636.
[18] E.S. Lee, E. de Josselin de Jong, H.I. Jung, B.I. Kim, Red fluorescence of dental biofilm as an indicator for assessing the efficacy of antimicrobials, J. Biomed. Opt. 23 (1) (2018) 1–6, https://doi.org/10.1117/1.Jbo.23.1.015003.
[19] E.S. Lee, M.Y. Cho, E. de Josselin de Jong, H.C. Yoon, I. KB, Classification of maturation of bacterial dental deposits using differences in fluorescence intensity, Korean Dent. Assoc. 57 (4) (2019) 213–220.
[20] W. Buchalla, A.M. Lennon, T. Attin, Fluorescence spectroscopy of dental calculus, J. Periodontal. Res. 39 (5) (2004) 327–332, https://doi.org/10.1111/j.1600-0765.2004.00747.x.
[21] B.B. Partido, C.A. Webb, M.P. Carr, Comparison of calculus detection among dental hygienists using an explorer and ultrasonic insert, Int. J. Dent. Hyg. 17 (2) (2019) 192–198, https://doi.org/10.1111/idh.12388.
[22] B.B. Partido, A.A. Jones, D.L. English, C.A. Nguyen, M.E. Jacks, Calculus detection calibration among dental hygiene faculty members utilizing dental endoscopy: a pilot study, J. Dent. Educ. 79 (2) (2015) 124–132.
[23] K.V. Garland, K.J. Newell, Dental hygiene faculty calibration in the evaluation of calculus detection, J. Dent. Educ. 73 (3) (2009) 383–389.
[24] M. Masud, H.I.M. Zahari, A.S.N. Sameon, N.A.H. Mohamed, Manual and electronic detection of subgingival calculus: reliability and accuracy, GSTF. J. Adv. Med. Res. 1 (8) (2014) 52–56, https://doi.org/10.7603/s40782-014-0008-7.
[25] J.I. Lee, M.J. Jeon, E.J. de Jong, H.I. Jung, I.Y. Jung, J.W. Park, et al., Evaluation of the clinical efficacy of quantitative light-induced fluorescence technology in diagnosing cracked teeth, Photodiagnosis. Photodyn. Ther. 41 (2023) 103299, https://doi.org/10.1016/j.pdpdt.2023.103299.
[26] S.H. Oh, J.Y. Choi, S.H. Kim, Evaluation of dental caries detection with quantitative light-induced fluorescence in comparison to different field of view devices, Sci. Rep. 12 (1) (2022) 6139, https://doi.org/10.1038/s41598-022-10126-x.
[27] D.T. Lindsey, A.G. Wee, Perceptibility and acceptability of CIELAB color differences in computer-simulated teeth, J. Dent. 35 (7) (2007) 593–599, https://doi.org/10.1016/j.jdent.2007.03.006.
[28] H.S. Lee, E.S. Lee, H.I. Jung, B.I. Kim, Distinguishing discolored caries lesions using biofluorescence and dental bleaching: an in vitro simulation model study, Photodiagnosis. Photodyn. Ther. 48 (2024) 104262, https://doi.org/10.1016/j.pdpdt.2024.104262.
[29] S. Dias, J. Dias, R. Pereira, J. Silveira, A. Mata, D. Marques, Different methods for assessing tooth colour-In vitro study, Biomimetics. (Basel) 8 (5) (2023), https://doi.org/10.3390/biomimetics8050384.
[30] C. Gómez-Polo, J. Montero, M. Gómez-Polo, A.M. Casado, Comparison of the CIELab and CIEDE 2000 color difference formulas on gingival color space, J. Prosthodont. 29 (5) (2020) 401–408, https://doi.org/10.1111/jopr.12717.
[31] S. Paul, A. Peter, N. Pietrobon, C.H. Hämmerle, Visual and spectrophotometric shade analysis of human teeth, J. Dent. Res. 81 (8) (2002) 578–582, https://doi.org/10.1177/154405910208100815.
[32] E.H. Jung, E.S. Lee, H.I. Jung, S.M. Kang, E. de Josselin de Jong, B.I. Kim, Development of a fluorescence-image scoring system for assessing noncavitated occlusal caries, Photodiagnosis. Photodyn. Ther. 21 (2018) 36–42, https://doi.org/10.1016/j.pdpdt.2017.10.027.
[33] V. Archana, Calculus detection technologies: where do we stand now? J. Med. Life (2014) 18–23, 7 Spec No. 2 (Spec Iss 2).
[34] F. Shakibaie, L.J. Walsh, Dental calculus detection using the VistaCam, Clin. Exp. Dent. Res. 2 (3) (2016) 226–229, https://doi.org/10.1002/cre2.42.
[35] H.J. Kim, E.S. Lee, B.I. Kim, Efficient gingival health screening using biofluorescence of anterior dental biofilms, Photodiagnosis. Photodyn. Ther. 53 (2025) 104546, https://doi.org/10.1016/j.pdpdt.2025.104546.
[36] S. Park, E.S. Lee, A. Kim, H.J. Kim, J.Y. Lee, S.K. Kim, et al., Development of a novel tongue biofilm index using bacterial biofluorescence, Sci. Rep. 14 (1) (2024) 30196, https://doi.org/10.1038/s41598-024-80696-5.
[37] S.W. Park, E.S. Lee, S.K. Kim, H.I. Jung, B.I. Kim, Quantitative assessment of early caries lesion activity using novel dye-enhanced fluorescence imaging, J. Dent. 150 (2024) 105352, https://doi.org/10.1016/j.jdent.2024.105352.
[38] S.M. Nam, H.M. Ku, E.S. Lee, B.I. Kim, Detection of pit and fissure sealant microleakage using quantitative light-induced fluorescence technology: an in vitro study, Sci. Rep. 14 (1) (2024) 9066, https://doi.org/10.1038/s41598-024-59651-x.
[39] A. Slimani, F. Nouioua, I. Panayotov, N. Giraudeau, K. Chiaki, Y. Shinji, et al., Porphyrin and pentosidine involvement in the red fluorescence of enamel and dentin caries, Int. J. Experim. Dental Sci. 5 (1) (2016) 1–10, https://doi.org/10.5005/jp-journals-10029-1115.
[40] R.M. Davies, R.P. Ellwood, A.R. Volpe, M.E. Petrone, Supragingival calculus and periodontal disease, Periodontol. 2000 15 (1997) 74–83, https://doi.org/10.1111/j.1600-0757.1997.tb00107.x.
[41] N.N. Moolya, S. Thakur, S. Ravindra, S.B. Setty, R. Kulkarni, K. Hallikeri, Viability of bacteria in dental calculus - A microbiological study, J. Indian Soc. Periodontol. 14 (4) (2010) 222–226, https://doi.org/10.4103/0972-124x.76921.
[42] C.M. Volgenant, E. Zaura, B.W. Brandt, M.J. Buijs, M. Tellez, G. Malik, et al., Red fluorescence of dental plaque in children -A cross-sectional study, J. Dent. 58 (2017) 40–47, https://doi.org/10.1016/j.jdent.2017.01.007.
[43] M.H. van der Veen, R.Z. Thomas, M.C. Huysmans, J.J. de Soet, Red autofluorescence of dental plaque bacteria, Caries Res. 40 (6) (2006) 542–545, https://doi.org/10.1159/000095655.
[44] W. Li, Y. Liang, X. Zhang, C. Liu, L. He, L. Miao, et al., A deep learning approach to automatic gingivitis screening based on classification and localization in RGB photos, Sci. Rep. 11 (1) (2021) 16831, https://doi.org/10.1038/s41598-021-96091-3.
[45] C. Wang, R. Zhang, X. Wei, L. Wang, W. Xu, Q. Yao, Machine learning-based automatic identification and diagnosis of dental caries and calculus using hyperspectral fluorescence imaging, Photodiagnosis. Photodyn. Ther. 41 (2023) 103217, https://doi.org/10.1016/j.pdpdt.2022.103217.